Applied Surface Science 392 (2017) 768–776

Contents lists available at ScienceDirect

Applied Surface Science

journal homepage: www.elsevier.com/locate/apsusc

Full Length Article

Anti-corrosion film formed on HAl77-2 copper alloy surface by aliphatic polyamine in 3 wt.% NaCl solution

Yinzhe Yu, Dong Yang, Daquan Zhang*, Yizhen Wang, Lixin Gao

Shanghai Key Laboratory of Materials Protection and Advanced Materials in Electric Power, School of Environment and Chemical Engineering, Shanghai University of Electric Power, Shanghai 200090, China

ARTICLE INFO

Article history:
Received 24 June 2016
Received in revised form
22 September 2016
Accepted 23 September 2016
Available online 25 September 2016

Keywords:
Copper alloy
Corrosion
Electrochemical measurements
SEM
AFM

ABSTRACT

The corrosion inhibition of a polyamine compound, *N*-(4-amino-2, 3-dimethylbutyl)-2, 3-dimethylbutane-1, 4-diamine (ADDD), was investigated for HAl77-2 copper alloy in 3 wt.% NaCl solution. Electrochemical measurements, scanning electron microscopy (SEM), atomic force microscope (AFM) and Fourier transform infrared spectroscopy (FT-IR) techniques were employed for this research. The results show that ADDD strongly suppresses the corrosion of HAl77-2 alloy. The inhibition efficiency of ADDD is 98.6% at 0.5 mM, which is better than benzotriazole (BTAH) at the same concentration. Polarization curves indicate that ADDD is an anodic type inhibitor. Surface analysis suggests that a protective film is formed via the interaction of ADDD and copper. FT-IR reveals that the inhibition mechanism of ADDD is dominated by chemisorption onto the copper alloy surface to form an inhibition film. Furthermore, quantum chemical calculation and molecular dynamics (MD) simulations methods show that ADDD adsorbs on HAl77-2 surface via amino group in its molecule.

1. Introduction

In recent years, research on copper alloy corrosion has got more attention in industrial sector [1,2]. Aluminum brass and copper-nickel alloy are widely used as tube materials for the heat-exchanger [3–5]. Copper alloy are susceptible to corrosion in seawater, which is one of the most corroded media [6–8]. The corrosion of copper alloy leads to many potential safety problems during the long operation process and causes tremendous economic losses in sea water environment [9,10]. The use of corrosion inhibitors in such conditions for copper alloy is necessary [11,12].

Numerous possible copper corrosion inhibitors have been investigated in the literature [13,14]. Among them, these aromatic heterocyclic compounds show a good corrosion inhibitive effect [15]. Benzotriazole (BTAH) is considered to be one of the most effective inhibitors for copper and its alloys [26]. There are some papers studying the effect of BTAH alone [16–18] and synergistic effect with other compounds such as potassium sorbate and Na_3PO_4 [19,20]. Many derivatives of BTAH are also investigated as copper inhibitors and display good inhibition efficiency [21–25]. However, toxicity is the major defect of BTAH and its derivatives. The use of BTAH is nowadays quite limited, especially in desalination industry. The replacement of BTAH with new environmentally friendly inhibitors is in urgent need.

Researchers make many efforts to develop green inhibitors such as amino acids, plant extracts, purine and natural products [27–30]. Our group also has investigated novel inhibitors, such as amino acids and peptides [31–34]. Aliphatic amine is often used as emulsifier in food processing, which is generally regarded as an environmental friendly substance.

In this paper, an aliphatic polyamine compound, *N*-(4-amino-2, 3-dimethylbutyl)-2, 3-dimethylbutane-1,4-diamine (ADDD), was used as a corrosion inhibitor for HAl77-2 copper alloy. The molecular structure of ADDD is shown in Fig. 1. The corrosion inhibition was evaluated by electrochemical impedance spectroscopy (EIS) and potentiodynamic polarization curves. It is found that ADDD is a better corrosion inhibitor for HAl77-2 copper alloy compared with BTAH at low concentration in chloride media. The scanning electron microscope (SEM), atomic force microscope (AFM) and Fourier transform infrared spectroscopy (FT-IR) were applied to analyze the corrosion surface. Quantum chemical calculation of density functional theory (DFT) was applied to study the inhibition mechanism.

2. Experimental

2.1. Materials and chemicals

The electrode used was made of HAl77-2 copper alloy plates (wt%: Cu 77.0, Al 2.0, As 0.05, Fe 0.06, Pd 0.06, Sb 0.05, Bi 0.02, P

* Corresponding author.
E-mail addresses: zhdq@sh163.net, zhangdaquan@shiep.edu.cn (D. Zhang).

http://dx.doi.org/10.1016/j.apsusc.2016.09.118
0169-4332/

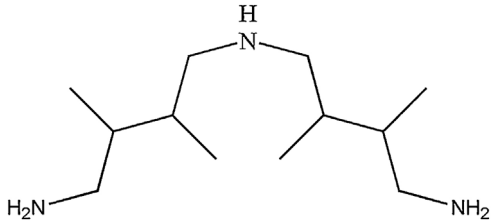

Fig. 1. Chemical structure of *N*-(4-amino-2, 3-dimethylbutyl)-2, 3-dimethylbutane-1, 4-diamine (ADDD).

0.02, and Zn balance). ADDD was supplied by Tianze Co. LTD. The epoxy was KD-504A type resin supplied by Cixi Tiandong adhesive factory Co. LTD. All other chemicals were of analytical grade and used as obtained.

To verify the complex film formed on copper alloy surface, the ADDD-Cu^{2+} complex was prepared by mixing ADDD solution with $CuCl_2$. Saturated solution of $CuCl_2$ (10 mL) was slowly added to the water solution (10 mL) of ADDD (0.5 mM) at 25 °C. The blue precipitate of the ADDD-Cu^{2+} complex was collected. The complex was characterized by FT-IR spectrum and compared with film that formed on the copper surface.

2.2. Electrochemical measurements

Electrochemical experiments were carried out in the conventional three-electrode cell with a platinum counter electrode (CE, exposure area greatly larger than WE's) and a saturated calomel electrode (SCE, Cl^- concentration 0.357 g/mL) as the reference electrode. The working electrode (WE) was sealed in an epoxy resin so that the exposure area was 0.5 cm^2. The WEs were gradually ground by emery paper down to #2000, and then degreased by AR grade ethanol. The electrochemical analysis was conducted on Solartron 1287 Electrochemical Interface coupled with a Solartron 1260 Impedance/Gain-Phase Analyzer. During the test, the cell was open to the air without stirred or deaerated. Electrochemical measurements were done at room temperature (25 °C) after 1 h immersion when the open circuit potential (OCP) was stable. EIS was measured at OCP in the frequency range from 0.01 Hz to 100 kHz with a 5 mV AC perturbation signal. The potential range of potentiodynamic polarization curves was from −400 to +600 mV (vs. E_{corr}) at a scan rate of 1 mV/s. All potential values in the paper were referred to SCE. The softwares of Zplot and CorrWare were employed to fit the data.

2.3. SEM imaging and EDS characterization

Copper alloy specimens were ground by different grades of emery paper (#800, #1200 and #2000) and rinsed with AR grade ethanol and distilled water. After 4 days dipping in 3 wt.% NaCl solution without and with inhibitor at 25 °C, copper alloy samples were rinsed with deionized water, and then allowed to air dry. Scanning electron microscope (SU-1500, Hitachi Company) images under an accelerating voltage of 20 kV were taken to observe the surface microstructure of the samples. The composition of the surface complex film on specimens was recorded by an energy dispersive spectroscopy.

2.4. AFM images

An atomic force microscope (AFM, Agilent 5500) was employed to investigate the detailed surface changes of the copper alloy in the aggressive condition in the absence and presence of inhibitors. After 4 days immersion in 3 wt.% NaCl solution, the specimens were rinsed with distilled water and dried in air, and then AFM measurements were performed open to air.

2.5. FT-IR analysis

Infrared spectra (PerkinElmer Spectrum Two) were recorded in the range from 400 to 4000 cm^{-1}. All specimens were analyzed in the reflection mode. A background spectrum was recorded for a copper alloy sample without inhibitor treatment. The infrared light from FT-IR spectrometer bench was directed on the sample and spherical windows. The angle of incidence was 80°. The optical window was adopted in KBr standard and spectral resolution used 0.5 cm^{-1} as a standard. The subsequent spectrum was recorded in absorbance units (I_t/I_0), where I_t is the reflected intensity of the inhibitor-treated specimens and I_0 is the reflectivity of the background spectrum.

2.6. Quantum chemical calculations and molecular dynamics (MD) simulations

Quantum chemical calculations were performed with density functional theory (DFT) in Materials Studio 6.0 software. Geometrical optimization was carried out with the generalized gradient approximation (GGA) functional. MD simulations were performed with Discover molecular dynamics module program in Materials Studio 6.0 software from Accelrys Inc. CuO (1 1 0) plane was chosen to fabricate an appropriate supercell. After vacuum slab and optimized inhibitor molecules built, the adsorption system was built by layer builder to place the inhibitor layer to CuO (1 1 0). The adsorption system was optimized using COMPASS (condensed phase optimized molecular potentials for atomistic simulation studies) force field. Simulated annealing was performed from 5000 K to 10 K. The adsorption energy (E_{ads}) of the inhibitor molecule on the CuO (1 1 0) surface can be calculated as follows [35]:

$$E_{ads} = \left(E_{inh} + E_{surf}\right) - E_{total} \quad (1)$$

where E_{inh} and E_{surf} are the energies of the free inhibitor molecule and CuO (1 1 0) plane, respectively. E_{total} is the energy of CuO (1 1 0) plane together with inhibitor molecule adsorbed on the surface. The binding energy (E_{bin}) is the negative value of E_{ads} [36]:

$$E_{bin} = -E_{ads} \quad (2)$$

3. Result and discussion

3.1. EIS analysis

The Nyquist plots and Bode plots of HAl77-2 alloy immersed in 3 wt.% NaCl solution for 1 h with and without inhibitors are depicted in Fig. 2. Three-parallel samples were included in the experiment. As for the naked HAl77-2 alloy, Nyquist plot displays an obvious capacitive loop in the high frequency and Warburg impedance at the low frequency. Warburg impedance suggesting the dissolution of HAl77-2 alloy is controlled by the transport of dissolved oxygen to copper surface or the chloride-copper complexes from electrode interface to bulk solution [37,38]. With the inhibitors concentration increasing, the curves of Nyquist plots show a single capacitive. The difference general shape of the EIS curves indicates that the corrosion mechanism is changed after adding inhibitor [39].

Nyquist plots were fitted with appropriate equivalent circuits to obtain EIS parameters. In the EIS fitting, the two most commonly used circuit models were applied to analyze the Nyquist plots. Equivalent circuits with two time constants were suitable for the EIS fitting and the fitted error values were below 10% and the chi-square was below 10^{-4}. The Bode plots demonstrate two overlapped phase maxima over a wide frequency zone, indicating the